Supplementary Information

RbMo$_2$P$_3$O$_{14}$ with Large Birefringence Mainly Induced by Highly Distorted [MoO$_6$] in the Uncommon [Mo$_2$P$_3$O$_{14}$]$_\infty$ Layers

Rui Zhang [a], Xin Su[*a], Jie Zhang[b], Mingyao Xiong,[a] Yineng Huang[a]

[a] Xinjiang Laboratory of Phase Transitions and Microstructures in Condensed Matter Physics, College of Physical Science and Technology, Yili Normal University, Yining, Xinjiang 835000, China.

[b] Department of Physics, Changji University. Changji, Xinjiang 831100, China.

*Corresponding author E-mail: suxin_phy@sina.com

Table S1 Crystal data and structure refinement for $RbMo_2P_3O_{14}$.

Empirical formula	$\mathbf{RbMo_2P_3O_{14}}$
Formula weight	594.26
Crystal system, space group	Monoclinic, $P2_1$
a (Å)	8.0271(3)
b (Å)	6.3124(2), β=96.121 (10）
c (Å)	11.9022(4)
Volume (Å^3)	599.65(4)
Z, Calculated density	2, 3.291 g/cm^3
F(000)	556.0
Theta range for data collection	3.442 to 55.102
Index ranges	-10 $\leq$ h $\leq$ 10, -8 $\leq$ k $\leq$ 8, -15 $\leq$ I $\leq$ 15
Reflections collected / unique	12256
Independent reflections	2781 [R_{int} = 0.0363, R_{sigma}= 0.029]
Data / restraints / parameters	2781/1/182
Goodness-of-fit on F_o^2	1.059
Final R indices [$F_o^2 > 2\sigma(F_o^2)$][a]	R_1=0.0195, wR_2=0.0464
Final R indices (all data) [a]	R_1=0.0207, wR_2=0.0471
Largest diff. peak and hole (e Å^{-3})	0.63/-0.61
Flack parameter	0.422(10)

[a] $R_1 = \Sigma||F_o| - |F_c||/\Sigma|F_o|$ and $wR_2 = [\Sigma w(F_o^2 - F_c^2)^2/\Sigma wF_o^4]^{1/2}$ for $F_o^2 > 2\sigma(F_o^2)$.

Table S2 Atomic coordinates ($\times 10^4$) and equivalent isotropic displacement parameters ($\text{Å} \times 10^3$) for RbMo$_2$P$_3$O$_{14}$. U_{eq} is defined as one-third of the trace the orthogonalised U_{ij} tensor.

Atom	x	y	z	U$_{eq}$	BVS
Rb(1)	3166.7(9)	8213.9(13)	2379.4(5)	38.66(17)	1.05
Mo(1)	7195.7(5)	7360.8(5)	5205.0(3)	12.29(10)	6.20
Mo(2)	7275.8(5)	9696.2(6)	331.2(3)	14.99(10)	6.24
P(1)	8487.8(14)	2270(2)	4945.0(9)	11.7(2)	5.13
P(2)	9431.5(16)	1966(2)	2658.5(10)	13.7(3)	5.11
P(3)	8675.5(16)	4600(2)	735.8(9)	14.6(2)	5.19
O(1)	6269(5)	7571(8)	3878(3)	27.3(9)	2.02
O(2)	5689(6)	9866(10)	1145(4)	40.0(11)	2.04
O(3)	5585(5)	7219(8)	5989(3)	22.6(8)	1.93
O(4)	7531(5)	4228(6)	5210(3)	21.7(10)	2.25
O(5)	7635(5)	446(6)	5482(3)	18.1(8)	2.17
O(6)	10312(4)	2412(7)	5330(3)	17.1(7)	1.91
O(7)	8212(4)	1887(7)	3612(3)	21.7(8)	2.16
O(8)	11188(5)	2073(7)	3160(3)	21.2(8)	1.99
O(9)	9046(6)	199(6)	1851(3)	23.7(10)	2.15
O(10)	8874(5)	4138(6)	2061(3)	20.5(8)	2.17
O(11)	10384(6)	4661(9)	376(4)	38.7(11)	2.03
O(12)	7587(6)	2866(7)	171(3)	26.8(11)	1.92
O(13)	7729(6)	6659(6)	627(3)	23.1(9)	1.98
O(14)	6257(6)	9491(8)	-967(4)	38.7(12)	2.18

Table S3 Selected bond distances (Å) and angles (deg.) for RbMo$_2$P$_3$O$_{14}$.

Rb(1)-O(1)	2.933(4)	Mo(2)-O(13)	1.976(4)
Rb(1)-O(2)	2.825(5)	Mo(2)-O(2)	1.684(4)
Rb(1)-O(9)#7	3.530(4)	Mo(2)-O(11)#5	2.139(4)
Rb(1)-O(12)#4	3.040(4)	Mo(2)-O(14)	1.675(4)
Rb(1)-O(4)#6	3.049(4)	P(1)-O(6)	1.489(3)
Rb(1)-O(5)#6	3.209(4)	P(1)-O(4)	1.506(4)
Rb(1)-O(3)#6	3.279(4)	P(1)-O(5)	1.515(4)
Rb(1)-O(8)#7	3.104(4)	P(1)-O(7)	1.597(4)
Rb(1)-O(14)#8	2.954(5)	P(2)-O(9)	1.484(4)
Mo(1)-O(6)#2	2.164(4)	P(2)-O(7)	1.576(4)
Mo(1)-O(4)	1.996(4)	P(2)-O(8)	1.473(4)
Mo(1)-O(5)#3	2.001(4)	P(2)-O(10)	1.587(4)
Mo(1)-O(3)	1.676(4)	P(3)-O(12)	1.512(4)
Mo(1)-O(1)	1.678(4)	P(3)-O(13)	1.504(4)
Mo(1)-O(8)#2	2.228(3)	P(3)-O(11)	1.480(5)
Mo(2)-O(9)#3	2.201(4)	P(3)-O(10)	1.595(4)
Mo(2)-O(12)#3	2.028(4)		
O(6)#1-Mo(1)-O(8)#1	77.75(13)	O(1)-Rb(1)-O(9)#8	151.19(11)
O(4)-Mo(1)-O(6)#1	83.53(17)	O(1)-Rb(1)-O(12)#4	131.54(12)
O(4)-Mo(1)-O(5)#3	160.56(15)	O(1)-Rb(1)-O(4)#6	71.69(11)
O(4)-Mo(1)-O(8)#1	81.43(17)	O(1)-Rb(1)-O(5)#6	70.81(12)
O(5)#3-Mo(1)-O(6)#1	83.20(17)	O(1)-Rb(1)-O(3)#6	63.92(12)
O(5)#3-Mo(1)-O(8)#1	81.92(17)	O(1)-Rb(1)-O(8)#8	110.78(11)
O(3)-Mo(1)-O(6)#1	163.23(15)	O(1)-Rb(1)-O(14)#7	93.53(13)
O(3)-Mo(1)-O(4)	93.3(2)	O(2)-Rb(1)-O(9)#8	119.07(13)
O(3)-Mo(1)-O(5)#3	95.4(2)	O(2)-Rb(1)-O(12)#4	65.44(14)
O(3)-Mo(1)-O(1)	103.73(19)	O(2)-Rb(1)-O(4)#6	128.73(14)
O(3)-Mo(1)-O(8)#1	85.50(16)	O(2)-Rb(1)-O(5)#6	146.02(13)
O(1)-Mo(1)-O(6)#1	93.01(17)	O(2)-Rb(1)-O(3)#6	80.37(14)
O(1)-Mo(1)-O(4)	97.3(2)	O(2)-Rb(1)-O(1)	76.02(13)
O(1)-Mo(1)-O(5)#3	97.5(2)	O(2)-Rb(1)-O(8)#8	106.50(14)
O(1)-Mo(1)-O(8)#1	170.75(17)	O(2)-Rb(1)-O(14)#7	80.40(16)
O(12)#3-Mo(2)-O(9)#3	81.93(15)	O(8)#8-Rb(1)-O(9)#8	43.56(9)
O(12)#3-Mo(2)-O(11)#5	81.4(2)	O(8)#8-Rb(1)-O(5)#6	92.14(10)
O(13)-Mo(2)-O(9)#3	84.43(16)	O(8)#8-Rb(1)-O(3)#6	49.57(10)
O(13)-Mo(2)-O(12)#3	162.15(17)	O(14)#7-Rb(1)-O(9)#8	112.43(11)
O(13)-Mo(2)-O(11)#5	84.7(2)	O(14)#7-Rb(1)-O(12)#4	53.19(12)
O(2)-Mo(2)-O(9)#3	88.9(2)	O(14)#7-Rb(1)-O(4)#6	139.28(12)
O(2)-Mo(2)-O(12)#3	95.7(3)	O(14)#7-Rb(1)-O(5)#6	94.31(12)
O(2)-Mo(2)-O(13)	95.5(2)	O(14)#7-Rb(1)-O(3)#6	153.34(12)
O(2)-Mo(2)-O(11)#5	167.7(2)	O(14)#7-Rb(1)-O(8)#8	155.62(11)
O(11)#5-Mo(2)-O(9)#3	78.92(18)	O(6)-P(1)-O(4)	113.1(2)

O(14)-Mo(2)-O(9)#3	168.1(2)	O(6)-P(1)-O(5)	112.9(2)
O(14)-Mo(2)-O(12)#3	92.45(19)	O(6)-P(1)-O(7)	110.0(2)
O(14)-Mo(2)-O(13)	98.7(2)	O(4)-P(1)-O(5)	105.8(2)
O(14)-Mo(2)-O(2)	102.1(3)	O(4)-P(1)-O(7)	108.2(2)
O(14)-Mo(2)-O(11)#5	89.9(2)	O(5)-P(1)-O(7)	106.4(2)
O(12)#4-Rb(1)-O(9)#8	76.38(11)	O(9)-P(2)-O(7)	109.9(2)
O(12)#4-Rb(1)-O(4)#6	156.64(11)	O(9)-P(2)-O(10)	109.26(19)
O(12)#4-Rb(1)-O(5)#6	135.86(13)	O(7)-P(2)-O(10)	100.5(2)
O(12)#4-Rb(1)-O(3)#6	131.52(11)	O(8)-P(2)-O(9)	114.9(3)
O(12)#4-Rb(1)-O(8)#8	107.58(11)	O(8)-P(2)-O(7)	110.5(2)
O(4)#6-Rb(1)-O(9)#8	80.26(10)	O(8)-P(2)-O(10)	110.7(2)
O(4)#6-Rb(1)-O(5)#6	45.19(10)	O(12)-P(3)-O(10)	107.4(2)
O(4)#6-Rb(1)-O(3)#6	49.91(10)	O(13)-P(3)-O(12)	108.9(2)
O(4)#6-Rb(1)-O(8)#8	53.30(10)	O(13)-P(3)-O(10)	103.8(2)
O(5)#6-Rb(1)-O(9)#8	94.09(10)	O(11)-P(3)-O(12)	113.6(3)
O(5)#6-Rb(1)-O(3)#6	91.40(10)	O(11)-P(3)-O(13)	115.3(3)
O(3)#6-Rb(1)-O(9)#8	93.06(9)	O(11)-P(3)-O(10)	107.0(2)

Symmetry transformations used to generate equivalent atoms:

#1 2-X,1/2+Y,1-Z	#2 1-X,-1/2+Y,1-Z
#3 +X,1+Y,+Z	#4 1-X,1/2+Y,-Z
#5 2-X,1/2+Y,-Z	#6 1-X,1/2+Y,1-Z
#7 -1+X,1+Y,+Z	#8 1-X,-1/2+Y,-Z

Table S4. Detailed contributions from the $[MoO_6]$, $[PO_4]$ and $[RbO_9]$ as well as the total polarization of the whole unit cell in the $RbMo_2P_3O_{14}$ compound.

Species		Dipole moment			
		x	y	z	Magnitude
$[Mo(1)O_6]$		1.854	-0.747	3.024	3.456
$[Mo(2)O_6]$		1.734	1.451	0.208	2.254
$[P(1)O_4]$		-2.050	-0.489	-0.719	2.155
$[P(2)O_4]$		-2.504	2.043	0.481	3.306
$[P(3)O_4]$		-0.968	-0.223	2.865	3.128
$[Rb(1)O_9]$		1.452	3.286	3.004	4.583
Unit cell	$\Sigma[MoO_6]$	-0.006	1.414	0.002	**1.414**
	$\Sigma[PO_4]$	0.003	2.660	-0.001	**2.660**
Z=2	$\Sigma[RbO_9]$	0	6.572	0	**6.572**
	Total polarization	**-0.003**	**10.646**	**0.001**	**10.646**
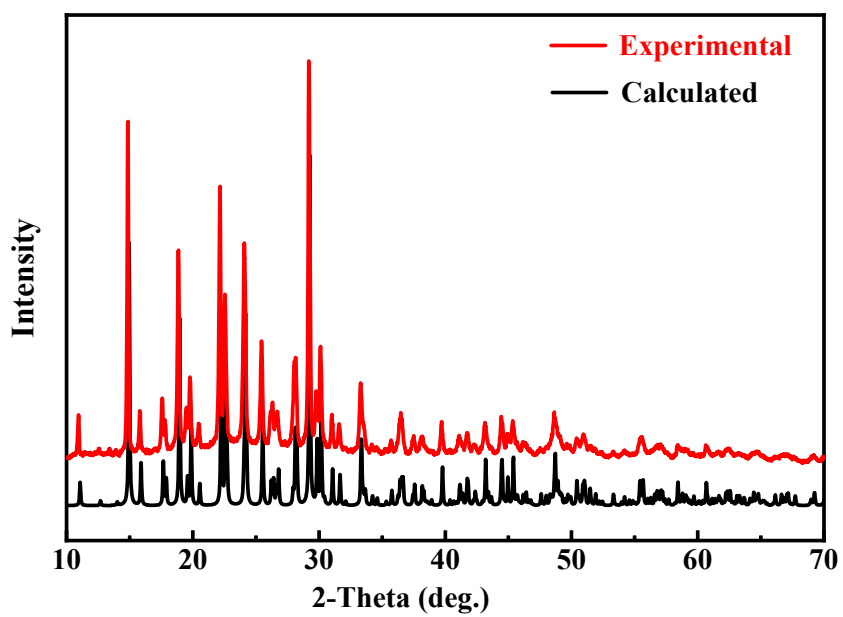
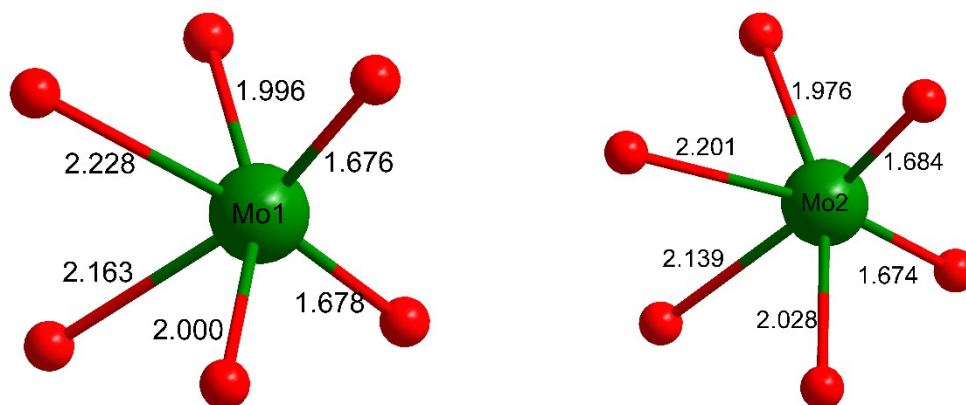Figure S1. The XRD patterns of $RbMo_2P_3O_{14}$.

Figure S2. The bond lengths of Mo-O in [MoO$_6$] octahedron.

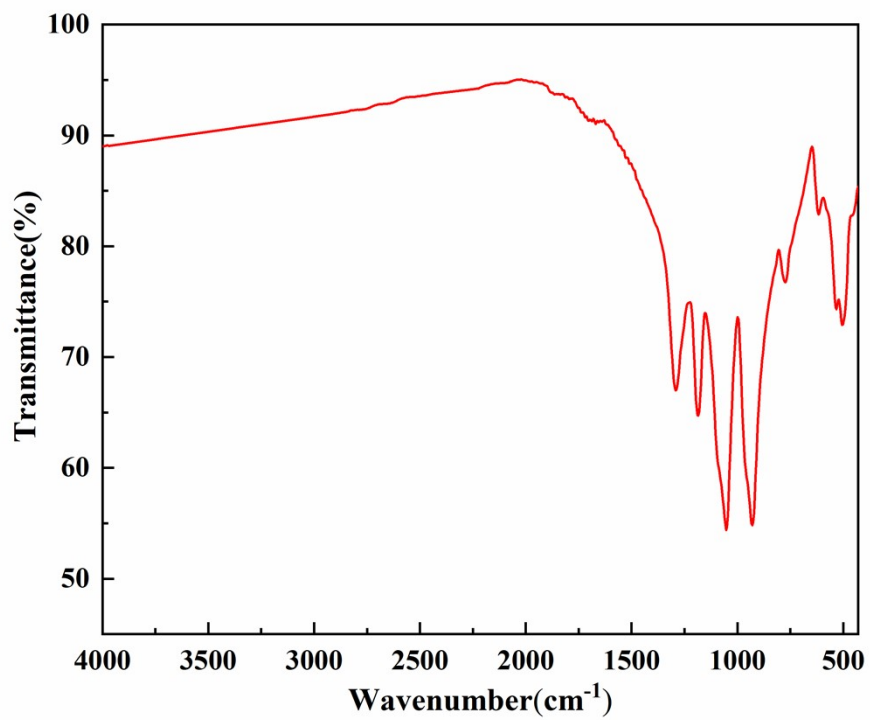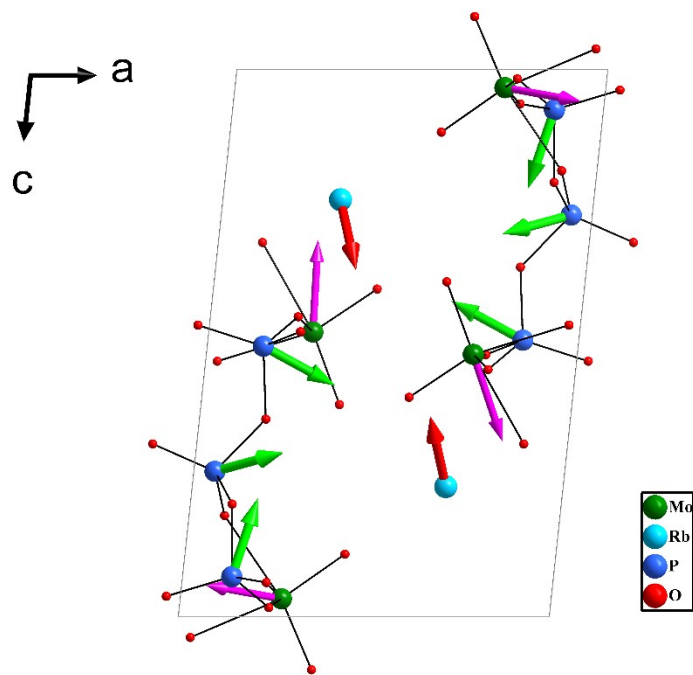Figure S3. The IR spectrum of $RbMo_2P_3O_{14}$.

Figure S4. The orientations of dipole moment for [MoO$_6$], [PO$_4$] and [RbO$_9$] polyhedra in RbMo$_2$P$_3$O$_{14}$.
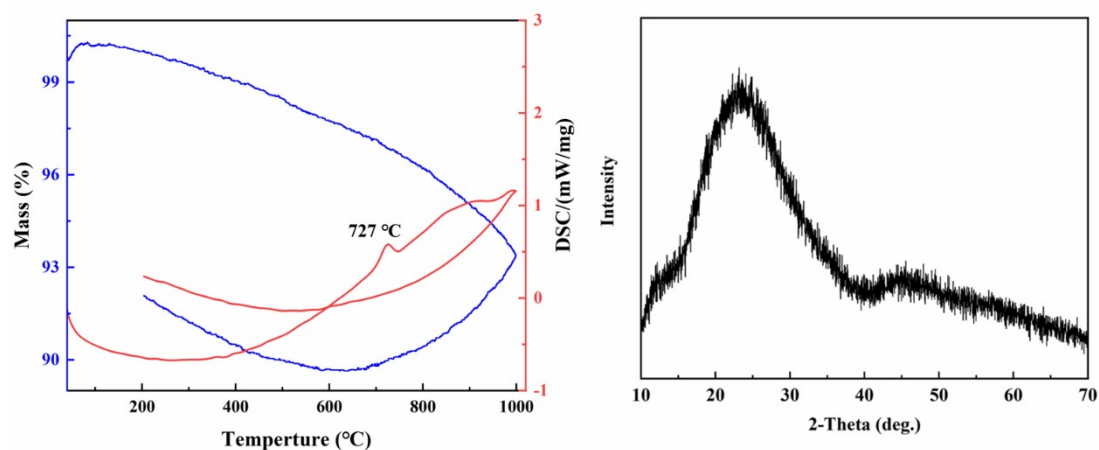
Figure S5. The melting behavior of $RbMo_2P_3O_{14}$ was carried out on NETZSCH STA 449C simultaneous analyzer instrument. The sample and reference, Al_2O_3, were

enclosed in Pt crucibles, heated from 40 to 1000 ℃ at a heating rate of 10 ℃/ min under

flowing nitrogen gas. Differential thermal analysis shows that there is only one endothermic peak on the heating DSC curve, along with weight loss on the TG curve (Left). There is no obvious exothermic peak in the whole cooling process due to the excessive viscosity of sample. The measurement indicates that $RbMo_2P_3O_{14}$ may decompose before melting, and it may melt incongruently. Furthermore, to testify to this initial conclusion, $RbMo_2P_3O_{14}$ polycrystalline sample was melted in a platinum crucible and recrystallized. The powder XRD pattern of recrystallized substance was glassy state due to its excessive viscosity (Right).